Available online at www.sciencedirect.com
SCIENCE DIRECT®
Ultrasonics Sonochemistry 10 (2003) 65–69
Ultrasonics SONOCHEMISTRY
www.elsevier.com/locate/ultsonch

Electrochemical detection of bubble oscillation

Yvonne E. Watson [a], Peter R. Birkin [a,*], Timothy G. Leighton [b]

[a] Department of Chemistry, University of Southampton, Highfield, Southampton SO17 1BJ, UK
[b] ISVR, University of Southampton, Highfield, Southampton SO17 1BJ, UK

Received 18 July 2002; accepted 14 November 2002

Abstract

The interaction of a tethered bubble with sound is demonstrated using novel electrochemical characterisation technology. A 25 μm diameter microelectrode, positioned close to the gas/liquid interface is used to monitor the motion of the bubble wall as a function of time in the presence and absence of sonic irradiation. Evidence for 'breathing' mode oscillation of the bubble and its effect on mass transfer to the microelectrode is presented.

Keywords: Bubble; Oscillation; Microelectrode; Surface waves

1. Introduction

The interaction of sound with gas bubbles within liquids is inherent in the generation of noise from many water motion based processes. For example, the sounds of a dripping tap, a waterfall and waves breaking have all been shown to be caused by the oscillations of the myriad of bubbles entrapped within the liquid phase [1]. In turn the interaction of bubbles in liquids with sound has been the subject of an intense research area with important applications ranging from sonochemistry [2–5] to medical imaging [6] and treatment [7–9]. In many of these areas the strong acoustic nature of a gas bubble enables the study to be performed in a passive sense (e.g. the monitoring of underwater noise). However, in other circumstances irradiation of the liquid with one or more sound waves can yield important information on the nature of the bubble environment under exploration. As an example Leighton et al. have pioneered the nonlinear investigation of the bubble population produced by breaking waves in the ocean [10–12]. In two of these investigations a combination frequency technique was employed [13–15]. This technique relies on excitation of bubble oscillation with a pump frequency (ω_p) and detection of the associated bubble oscillations with an imaging high frequency sound wave (ω_i). Bubble oscillation could be detected as frequency components at $\omega_i \pm \omega_p$ and $\omega_i \pm \omega_p/2$ within the scattered imaging beam from the oscillating gas body. These different frequency components reflect the number of different (and sometimes simultaneous) modes of oscillation, which the bubble wall can undergo when excited by a sound field. In the first example the bubble can pulsate or 'breath' spherically symmetrically [16]. This breathing mode is responsible for the strong acoustic emission into the liquid phase when bubbles are entrapped. However, there is a second common form of bubble oscillation that can be broadly classed as surface waves [16]. For the amplitudes of sound fields employed in this paper, surface waves have wall displacement amplitudes of the order of 75 μm compared to ≈3 μm displacements usually associated with the volumetric breathing mode pulsation. This surface wave phenomena is responsible for the 'shimmering' observed when a gas bubble is driven into oscillation by a suitable acoustic pressure field. The breathing mode and the surface wave modes of oscillation of a gas bubble pose contradictory characteristics. Being a monopole the breathing mode, although small (here ≈3 μm) is highly acoustically active. In contrast the surface waves, although characterised by much larger wall displacements, which are easily observed using photographic technology, are difficult to detect acoustically. This interesting paradox in behaviour

* Corresponding author. Fax: +44-23-80-593781.
E-mail address: prb2@soton.ac.uk (P.R. Birkin).

1350-4177/02/$ - see front matter © 2002 Elsevier Science B.V. All rights reserved.
PII: S1350-4177(02)00149-9

has driven research into complex forms of acoustic characterisation such as the combination frequency study described above [13–15] where the $\omega_i \pm \omega_p$ signal is generated by the breathing mode, which is always present if the bubble is being driven. In contrast the $\omega_i \pm \omega_p/2$ is a threshold phenomena, dependant on the amplitude and frequency of the driving field. This is because the surface waves are threshold phenomena; the one which takes the lowest driving pressure to excite, is that mode having a natural frequency close to $\omega_p/2$. This first surface wave to be excited (at half the driving frequency) is called the Faraday wave.

While the oscillation of a gas bubble within a liquid can be difficult to characterise acoustically, it has been shown that the motion of gas bubbles in liquids can be followed using electrochemistry. As an example Whitney and Tobias used a micromosaic electrode to study the effect of a bubble rising under buoyancy forces on mass transfer to an electrode [17]. In particular these studies were designed to distinguish between the differing mechanisms thought to be responsible for mass transfer enhancement in the liquid phase due to buoyant bubble motion (no sound field was applied). However, if electrochemistry can be used to monitor mass transfer enhancements due to buoyancy, then it should also be possible to detect the motion of the liquid surrounding an oscillating gas bubble. This has been demonstrated for a tethered bubble driven to oscillate by an appropriate acoustic field [18,19]. In this novel technique the motion of the gas liquid interface was monitored by observing the current as a function of time at a 25 μm diameter Pt microelectrode positioned close to the gas/liquid boundary of a tethered gas bubble. In the absence of bubble oscillation the mass transfer of material to the microelectrode is driven by diffusion alone. However, when surface waves were initiated on the gas bubble by acoustic excitation, the mass transfer to the microelectrode was enhanced due to the additional convection of the liquid around the oscillating bubble. This mass transfer enhancement could be detected at a significant distance (up to 2.5 mm) from the gas liquid interface [18] and was shown to be caused by Faraday wave [19] motion of the bubble.

Although electrochemical evidence for Faraday wave motion of the bubble wall has been presented previously, it will be shown here that the detection of the much smaller fundamental or breathing mode of bubble oscillation in the absence of Faraday wave motion is possible using the same electrochemical technique.

2. Experimental

The experimental set-up has been described previously [18,19]. All pressures were measured in the absence of the bubble unless otherwise stated. A Kodak HS 4540 high-speed camera was used to record images of bubbles of differing radii driven into oscillation by an applied sound field. The system records at 4500 frames per second (fps) with a full size picture and up to 40,500 fps with reduced picture size. The system records 3072 full frames, so that at 4500 fps, recording time of 0.66 s is available. The resolution of the system is 256×256 pixels. A monozoom lens was used to focus the required images.

The cell in the experimental set-up was described previously [19]. However, small mirrors were positioned around the cell to maximise the amount light entering the cell via a spotlight. The position of the camera was adjusted until a clear image was seen on the TV monitor attached to the camera. Recording rates of 4500 and 9000 fps were used to capture the images. Each individual image was then stored on the VHS video recorder over a longer timescale so that blocks of frames could be viewed at a later date. Individual frames or groups of frames were also transferred to a PC.

$K_3[Fe(CN)_6]$ (Sigma, 99.5%) and $Sr(NO_3)_2$ (Aldrich, 99+%) were used as received. All solutions were made up using water purified through a USF Elga Option E10 water purification system.

3. Results and discussion

Fig. 1 shows an image of a gas bubble driven into surface wave oscillation by an acoustic driving signal. The image was gathered by a high-speed camera and recorded from below the bubble, which was restrained from rising under buoyancy by a glass rod [19]. Fig. 1

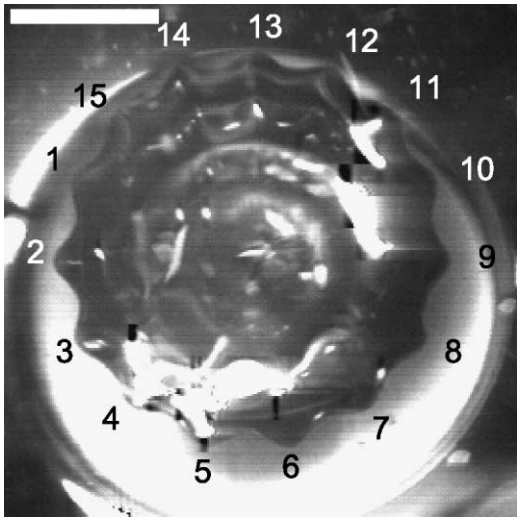

Fig. 1. Image recorded of a tethered gas bubble driven into oscillation by an acoustic driving field. Surface waves are clearly seen on the gas/liquid interface. The bubble was driven at 1.297 kHz. The scale bar represents 2 mm. The image is annotated to indicate the mode excited ($n = 15$).

clearly shows the presence of surface waves on the gas/liquid interface. From the number of peaks around the 'equator' of the bubble, the mode order is 15 [20]. The maximum displacement of the interface can be seen to be of the order of 75 μm as expected for surface wave phenomena. However, it was impossible to observe any breathing mode oscillation in this experimental set-up, as the amplitude of oscillation was too small as expected.

Fig. 2 shows how the current observed at a microelectrode varied as a function of frequency at a constant acoustic driving force (41 Pa amplitude). As the frequency was swept from 1.23 to 1.46 kHz with a constant driving pressure of ≈41 Pa the time averaged current (●) gradually rises until the frequency reaches 1.36 kHz where a sharp rise in current can be observed. This demarcation line coincides with the visual observation of 'shimmering' of the bubble wall and a component in the current time transient (observed on an oscilloscope) at $f_p/2$ (where f_p is the frequency of the acoustic drive signal). Since in super-threshold conditions it is known that the Faraday wave is excited only in a limited frequency band about the bubble resonance [20] this sharp rise is attributed to Faraday (surface) wave motion of the bubble wall reported previously [18,19]. The high current continued until the drive frequency reached 1.41 kHz where a sharp reduction in the current was observed. However, the current between 1.23 and 1.355 and 1.41 and 1.46 kHz does not reach the value measured in the absence of sound irradiation (∼−8 nA). Hence, it implies that the current measured at the microelectrode was enhanced by bubble motion other than that driven by surface wave phenomena. Clearly this enhancement in current is likely to be due to the breathing mode of the bubble wall because this is the only mode of oscillation to be excited considering the limited frequency range where it is possible to generate a Faraday wave. The demarcation between the breathing mode and the Faraday wave motion of the bubble wall is further illustrated by plotting on Fig. 2 the pressure threshold (○) for Faraday wave motion (as determined by monitoring the AC nature of the current recorded at the microelectrode on an oscilloscope and noting the conditions where a $f_p/2$ component was observed). This region coincides with the region in the frequency current plot where the sharp increase in the current was observed. The solid line on Fig. 2 (—) shows the predicted pressure threshold using a model reported previously [19]. Clearly the fit between the experimental data (○) and the prediction is reasonable particularly considering the experimental conditions employed to restrain the bubble.

In order to study the breathing mode in more detail the acoustic driving pressure was reduced below that expected to excite the Faraday wave motion on the bubble wall. Fig. 3 shows how the time averaged normalised current at a microelectrode positioned close to a bubble wall varied as a function of drive acoustic frequency for two different bubbles. In each case the time averaged normalised current enhancement was small in comparison to that expected for Faraday wave detection [18,19]. However, the current frequency plot is clearly smooth and has no sharp increases of the type shown in Fig. 2. In these two experiments, only the excitation of

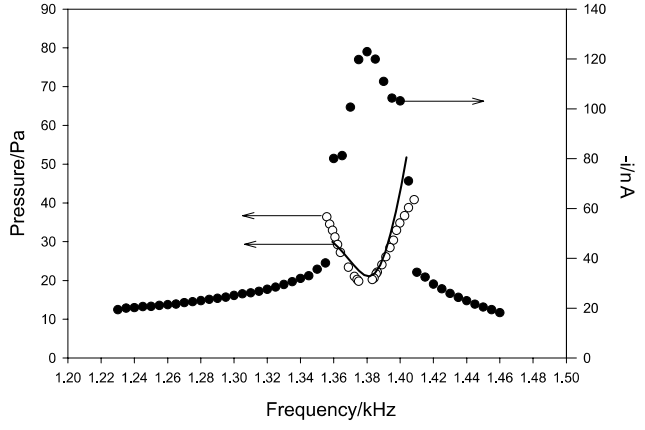

Fig. 2. Plot showing time averaged current recorded at a microelectrode positioned close (≈5–10 μm) from the gas/liquid interface of a air bubble plotted as a function of frequency (●). The aerobic aqueous solution contained 5 mmol dm^{-3} $K_3[Fe(CN)_6]$ in 0.2 mol dm^{-3} $Sr(NO_3)_2$. The 25 μm diameter Pt electrode was held at −0.1 V vs. Ag. The solution temperature was 20–23 °C and the acoustic pressure was 41 Pa. The pressure threshold for Faraday wave observation is also shown for interest (○). (—) represents the predicted threshold using a model reported previously ($n = 14$, $\sigma = 0.0685$ N m^{-1}) [19].

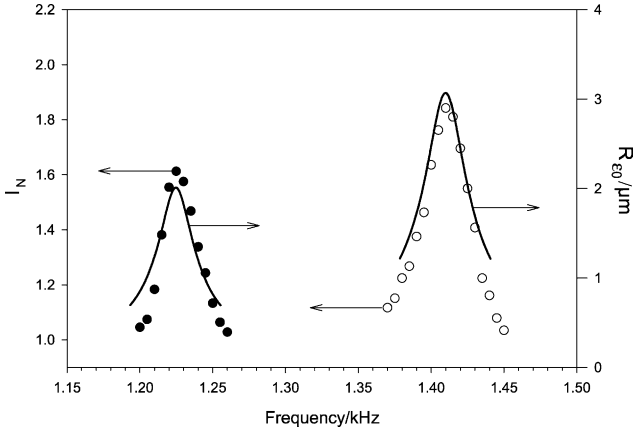

Fig. 3. Plot showing time averaged normalised current recorded for two air bubbles driven into oscillation below the threshold for Faraday wave excitation. In each case the excitation pressure was 5.8 and 10.4 Pa for (●) and (○) respectively. The solid lines indicate the estimated bubble wall displacement amplitude calculated under the conditions stated (see Ref. [1] Eq. (4.23)). The currents were normalised to the current recorded in the absence of sound irradiation (6.82 and 8.85 nA for (●) and (○) respectively). All other experimental conditions are described in Fig. 2.

the breathing mode was achieved and subsequently the currents are smaller but alter in a systematic way with respect to the applied acoustic drive frequency. The displacement amplitude (—), calculated using Eq. (4.23) Ref. [1], under the physical conditions employed in the experiment is included for both bubbles. This shows that the time average current follows closely the predicted wall displacement amplitude as expected.

Fig. 4a shows a series of results recorded at a sample rate of 50 kHz (sufficient to capture the AC nature of the current caused by bubble oscillation) for a tethered gas bubble excited by an acoustic driving signal. In this case the frequency was maintained at 1.167 kHz. Fig. 4a shows how the increasing acoustic pressure employed in the experiment enhanced the current. In addition at the higher pressures an AC signal can be seen on the current time traces. Consider the current time traces at the higher acoustic pressures (e.g. 20.3 Pa) compared to a pressure time trace recorded using a hydrophone placed in the same solution. It is evident that the AC modulation of the current occurs at the fundamental driving signal of the acoustic wave. This is further evidence that the current enhancement below 21 Pa was caused by the breathing mode of the bubble. Fig. 4b shows how the time average current varied as a function of the drive acoustic pressure. The current can be seen to steadily increase cathodically until a critical pressure amplitude was exceeded (≈21 Pa) where a rapid change in the current was observed. This corresponds to the excitation of the Faraday (surface) wave motion of the bubble wall. This was further confirmed by analysis of the AC component of the current recorded on an oscilloscope. Fig. 5 shows the current time relationship for 21.7 and 22.9 Pa driving pressure ($f_p = 1.167$ kHz). The current time behaviour occurs at $f_p/2$ in both cases and is indicative of surface wave subharmonic motion in agreement with previous studies [18,19].

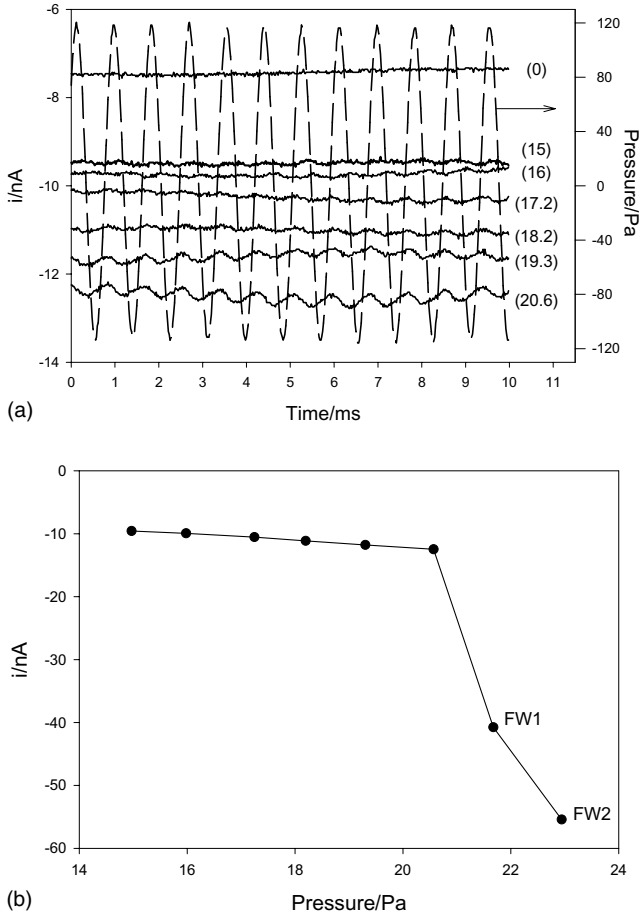

Fig. 4. (a) Plot showing the current (—) recorded as a function of time as the acoustic pressure was increased. The actual pressure amplitude measured in the absence of the bubble at which each current was recorded is given in the parenthesis in the figure next to the current time trace. (- - -) represents the acoustic pressure measured simultaneously in the presence of the bubble for reference. The acoustic driving signal was maintained at 1.167 kHz. All other experimental conditions are described in Fig. 2. (b) Plot showing the average current recorded for a single air bubbles driven into oscillation as a function of the acoustic driving pressure. The points labelled with 'FW' represent those experiments where Faraday waves were observed.

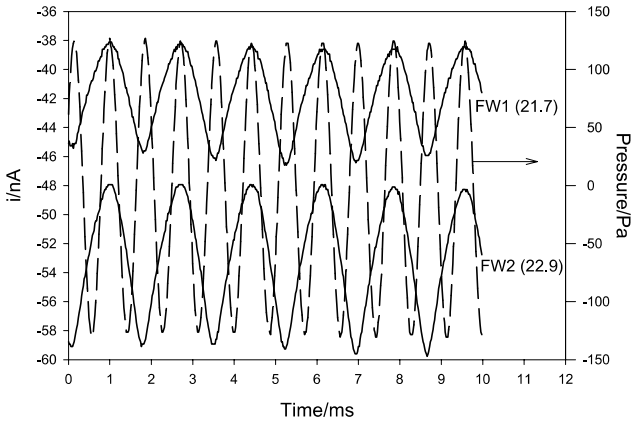

Fig. 5. Plot showing the current (—) for the Faraday wave electrochemical signals labelled 'FW' on Fig. 4b. (- - -) represents the acoustic pressure measured simultaneously in the presence of the bubble for reference. The acoustic pressure amplitudes are given in parenthesis while the drive frequency was maintained at 1.167 kHz. All other experimental conditions are described in Fig. 2.

4. Conclusions

The results show collectively that the motion of a tethered gas bubble irradiated with sound can be successfully investigated using a microelectrode positioned close to the gas/liquid interface. It is possible to detect the breathing mode oscillation of the bubble wall and surface wave oscillation of the gas/liquid interface depending on the pressure/frequency conditions. If the breathing mode is solely excited then the current enhancement can be seen to vary as both a function of

acoustic pressure and acoustic frequency. However, in this case relatively mild current enhancements were observed under the conditions employed but the current enhancement was detectable over a wider frequency range in comparison to Faraday wave motion of the bubble wall. The results are in agreement with dynamic theory of bubble walls.

Acknowledgements

The authors thank the EPSRC (Grant GR/M24615/01) for support. TGL would like to thank the Royal Society Leverhulme trust for a senior research fellowship.

References

[1] T.G. Leighton, The Acoustic Bubble, Academic Press, New York, 1994.
[2] P.R. Birkin, S.S. Martinez, J. Electroanal. Chem. 416 (1996) 127.
[3] P.R. Birkin, J.F. Power, T.G. Leighton, J. Chem. Soc. Chem. Commun. (2001) 2230.
[4] K. Makino, M.M. Mossoba, P. Reisz, J. Phys. Chem. 87 (1983) 1369.
[5] R.G. Compton, J.C. Eklund, S.D. Page, J. Appl. Electrochem. 26 (1996) 775.
[6] J. Ophir, K.J. Parker, Ultrasound Med. Biol. 15 (1989) 319.
[7] E.O. Belcher, IEEE Trans. Biomed. Engng. 27 (1980) 330.
[8] A.J. Coleman, M. Whitlock, T.G. Leighton, J.E. Saunders, Phys. Med. Biol. 38 (1993) 1545.
[9] A.J. Coleman, M.J. Choi, J.E. Saunders, T.G. Leighton, Ultrasound Med. Biol. 18 (1992) 267.
[10] A.D. Phelps, D.G. Ramble, T.G. Leighton, J. Acoust. Soc. Am. 101 (1997) 1981.
[11] A.D. Phelps, T.G. Leighton, IEEE J. Ocean Engng. 23 (1998) 400.
[12] T.G. Leighton, S.D. Meers, M.D. Simpson, J.W.L. Clarke, G.T. Yim, P.R. Birkin, Y.E. Watson, P.R. White, G.J. Heald, H.A. Dumbrell, R.L. Culver, S.D. Richards, Acoustical oceanography, in: T.G. Leighton, G.J. Heald, H. Griffiths, G. Griffiths (Ed.), Proceedings of the Institute of Acoustics, vol. 23, 2001, p. 227.
[13] T.G. Leighton, R.J. Lingard, A.J. Walton, J.E. Field, Ultrasonics 29 (1991) 319.
[14] T.G. Leighton, A.D. Phelps, D.G. Ramble, D.A. Sharp, Ultrasonics 34 (1996) 661.
[15] A.D. Phelps, T.G. Leighton, J. Acoust. Soc. Am. 99 (1996) 1985.
[16] P.R. Birkin, T.G. Leighton, Y.E. Watson, J.F. Power, Acoust. Bull. 26 (2001) 24.
[17] G.M. Whitney, C.W. Tobias, AIChE J. 34 (1988) 1981.
[18] P.R. Birkin, Y.E. Watson, T.G. Leighton, J. Chem. Soc. Chem. Commun. (2001) 2650.
[19] P.R. Birkin, Y.E. Watson, T.G. Leighton, K.L. Smith, Langmuir 18 (2002) 2135.
[20] A.O. Maksimov, T.G. Leighton, Acustica 87 (2001) 322.